The Astrophysical Journal, 699:L130–L133, 2009 July 10 doi:10.1088/0004-637X/699/2/L130

EVOLUTION OF THE RATE AND MODE OF STAR FORMATION IN GALAXIES SINCE $z = 0.7$

Alan Dressler[1], Augustus Oemler Jr.[1], Michael G. Gladders[2], Lei Bai[1], Jane R. Rigby[1], and Bianca M. Poggianti[3]
[1] The Observatories of the Carnegie Institution of Washington, 813 Santa Barbara Street, Pasadena, CA 91101-1292, USA; dressler@ociw.edu, oemler@ociw.edu, leibai@ociw.edu, jrigby@ociw.edu
[2] Department of Astronomy & Astrophysics, University of Chicago, Chicago, IL 60637, USA; gladders@uchicago.edu
[3] INAF-Osservatorio Astronomico di Padova, vicolo dell'Osservatorio 5, 35122 Padova, Italy; bianca.poggianti@oapd.inaf.it
Received 2009 April 2; accepted 2009 May 29; published 2009 June 22

ABSTRACT

We present the star formation rate (SFR) and starburst fraction (SBF) for a sample of field galaxies from the Inamori-Magellan Areal Camera and Spectrograph Cluster Building Survey intermediate-redshift cluster survey. We use [O II] and *Spitzer* 24 μm fluxes to measure SFRs, and 24 μm fluxes and Hδ absorption to measure SBFs, for both our sample and a present-epoch field sample from the Sloan Digital Sky Survey and *Spitzer* Wide-area Infrared Extragalactic survey. We find a precipitous decline in the SFR since $z = 1$, in agreement with other studies, as well as a corresponding rapid decline in the fraction of galaxies undergoing long-duration moderate-amplitude starbursts. We suggest that the change in both the rate and mode of star formation could result from the strong decrease since $z = 1$ of gas available for star formation.

Key words: galaxies: evolution – galaxies: starburst – galaxies: stellar content

1. INTRODUCTION

In recent years, much attention has been focused on the early history of star formation, in particular, the rise of the star formation rate (SFR) to its peak around $z \sim 2$ (e.g., Fall et al. 1996; Madau et al. 1998; Giavalisco et al. 1994; Pérez-González et al. 2008; Bouwens et al. 2008). Such a rapid rise is not surprising considering the dynamical timescales of galaxy-sized structures and the lifetimes of stars. More surprising, perhaps, is the precipitous decline in the global SFR since $z \approx 1$—more than a factor of 10 lower than its peak value, and falling fast (e.g., Lilly et al. 1996; Schiminovich et al. 2005; Hopkins & Beacom 2006; Villar et al. 2008). This is remarkable not only for its rapidity but also because it appears to mark our epoch as the beginning of the end of galactic star formation. It is now clear that the unexpected prevalence of star-forming galaxies in rich galaxy clusters discovered by Butcher & Oemler (1978), long regarded as a cluster phenomenon, is universal, as star-forming galaxies—great and small—surrender youthful vigor and fade toward oblivion in only a few billion years.

Using the wide field of the Inamori-Magellan Areal Camera and Spectrograph (IMACS) on Magellan-Baade, the IMACS Cluster Building Survey (ICBS) is focused on the study of galaxy infall and evolution from $R \sim 5$ Mpc into cluster cores. Because the projected density of cluster/supercluster members is low at such large radii, our near-complete samples necessarily include ~1000 "field" galaxies at redshift $0.2 < z < 0.8$ per survey field. This gives us an opportunity to compare galaxy evolution in clusters with the field over this epoch. From these data, we report in this Letter on the significant decline in SFR and starburst fraction (SBF) since $z \sim 1$.

2. DATA

The data discussed here come from four fields that contain rich galaxy clusters at $z = 0.33, 0.38, 0.42$, and 0.55. The IMACS $f/2$ spectra have an observed-frame resolution of 10 Å full width at half-maximum with a typical S/N ~ 20–30 in the continuum per resolution element. Spectral coverage varies, but almost all cover [O II] and Hβ emission, and Hδ absorption, our optical diagnostics of star formation; a fraction cover Hα as well. In each 28′ diameter IMACS field, we have observed 65% of the galaxies that are brighter than $r \sim 22.5$, obtaining adequate spectra of 81% of these. Measurement of spectral features followed procedures described in Dressler et al. (2004, hereinafter D04). For two fields we have confusion-limited MIPS 24 μm images (Guest Observer program 40387) that cover nearly the entire IMACS fields. Details of the data, data reduction, and analysis of the field sample are described in A. Oemler Jr. et al. (2009, in preparation).

In the following analysis, we include all galaxies between $0.10 < z < 0.70$ with absolute AB magnitudes at 4400 Å brighter than $M^*_{44} + 1.0$, except for those with redshifts within $\pm 3\sigma$ of each targeted cluster. M^*_{44} has been determined to evolve with redshift as $M^*_{44} = -20.00 - z$ (A. Oemler Jr. et al. 2009, in preparation); the limit of $M^*_{44} + 1.0$ is about equivalent to $r = 22.5$ at $z = 0.70$. There are 1144 objects in this sample. Galaxies are given weights proportional to the inverse of the incompleteness of the data at each apparent magnitude. To provide a low-redshift point, we use two samples of Sloan Digital Sky Survey (SDSS) galaxies with redshifts $0.04 < z < 0.08$. To compare to infrared-derived (IR-derived) properties of the ICBS sample, we use a sample of 385 SDSS galaxies within the SWIRE fields (Lonsdale et al. 2003). For comparison with the optically derived properties of our sample, we use this SDSS/SWIRE sample and add 690 SDSS galaxies near the north Galactic pole. We assume a concordance cosmology with $\Omega_{\rm matter} = 0.27$ and $H_0 = 71$ km s^{-1} Mpc^{-1}.

3. MEASUREMENTS OF SFR SINCE $z = 0.7$

For galaxies with *Spitzer*–MIPS coverage, we calculate SFRs in a way similar to Pérez-González et al. (2006), using the 24 μm flux to estimate the absorbed UV flux and [O II] to estimate the escaped UV flux, but including the k-corrections of Rieke et al. (2009) and an SFR scale based on a Salpeter initial mass function (IMF; vid. A. Oemler Jr. et al. 2009, in preparation). Donley et al. (2008) report that 10%–15% of 24 μm sources at these flux densities are active galactic nucleus (AGN)-dominated. Given the strong redshift evolution of the AGN luminosity function, the contamination in our $z < 0.7$ sample should be considerably lower. Figure 1 (bottom panel) shows the median SFR per unit L/L^*, which we shall refer to as the specific SFR, as a function of redshift. We choose the *median* specific SFR over the more

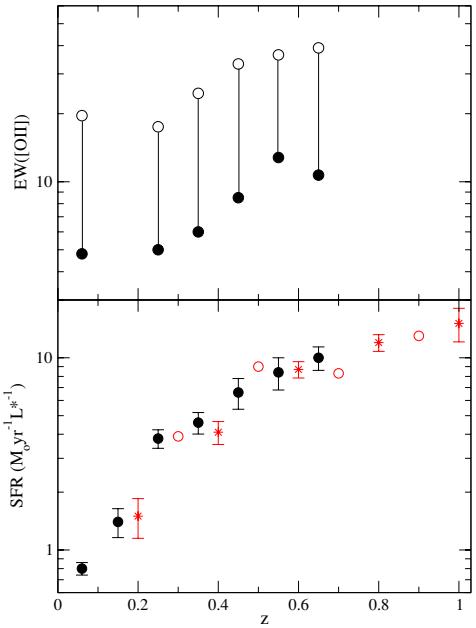

Figure 1. Bottom: *median* specific SFR, in solar masses per year per L^* luminosity. Black filled circles show values for our sample derived from *Spitzer*–MIPS 24 μm fluxes. Red stars are data from Damen et al. (2009), and red open circles are data from Pérez-González et al. (2008) as reinterpreted by Damen et al. (2009). The median SFR appears to be declining more rapidly toward the present epoch. Top: median values (solid circles) and 90th percentile values (open circles) of [O II] for the $z > 0.2$ ICBS field sample, binned to achieve comparable numbers of [O II]-detected galaxies. The single point at $z = 0.06$ comes SDSS galaxies with optical spectroscopy (see the text).

commonly reported *mean*, because it provides a more stable and typical value—particularly at higher redshifts, where the mean is dominated by a small number of very luminous objects. (In the $0.60 < z < 0.70$ interval, only 1.6% of the objects contribute 56% of the total star formation.) We also show, for comparison, values of the median SFR/(L/L^*), derived from the mid-IR data of Damen et al. (2009), and from the Pérez-González et al. (2008) study of the buildup of stellar mass (from near-IR measurements), as reinterpreted by Damen et al. and converted by us to a Salpeter IMF scale. To convert the Damen et al. values of SFR per unit mass to SFR/(L/L^*) we take a mean value of M/L at 4400 Å of 3, which is the ratio of the cosmic mass density (Pérez-González et al. 2008) to the cosmic luminosity density (Blanton et al. 2003). Although cosmic means, both are dominated by galaxies in the luminosity and mass ranges of our sample, and thus appropriate for our use. With $M/L = 3$, a sample with our absolute magnitude limit has a mean mass of $5 \times 10^{10}\, M_\odot$.

At $z > 0.4$ the *median* values of SFR increase more slowly than the mean SFR, as reported by Damen et al. (2009), Martin et al. (2007), and Zheng et al. (2007), but are otherwise qualitatively similar. However, what has not been apparent from previous observations is that the fall of the median SFR appears to be accelerating in recent epochs.

Optical emission lines [O II], Hβ, and Hα are less reliable SFR indicators than 24 μm flux because of the very large and variable extinction which blankets the H II regions of star-forming galaxies. However, they do provide at least a qualitative measure of current star formation and, unlike our *Spitzer*–MIPS data, are available for all four ICBS fields. Therefore, we plot in the top panel of Figure 1 the 50th and 90th percentiles of the distribution of *equivalent width* EW([O II]) as a function of redshift. The shapes of these distributions are qualitatively similar to the IR-derived SFR, however, [O II] strength increases more slowly with redshift because of the well known effect that galaxies with higher SFRs also have higher dust extinction.

4. WERE STARBURSTS THE NORMAL MODE OF STAR FORMATION BEFORE $z = 1$?

It is now well established that starburst and post-starburst galaxies are abundant in intermediate-redshift clusters (Poggianti et al. 1999, hereinafter P99; Oemler et al. 2009), however, less is known about the prevalence of starbursts among field galaxies at these epochs. Starburst indicators include exceptionally strong Balmer absorption, intense optical emission, and excess 24 μm flux. Strong Balmer absorption in the integrated light of galaxies signals a rapid decline in the SFR, because light from A stars persists after the blue continuum from O and B stars, and the emission from H II regions—both of which dilute the Balmer absorption lines—begin to fade or disappear altogether (P99). Although strong Balmer absorption accompanies even the simple truncation of star formation, as O and B stars and their H II regions evolve away, stellar EW(H$\delta \gtrsim 5$ Å occurs only in the aftermath of a significant rise in the SFR above its past average, i.e., a burst (Dressler & Gunn 1983; Couch & Sharples 1987, P99). Using this criterion, P99, D04, and Oemler et al. (2009) found that the SBF in the field at $z \sim 0.4$ is lower than in clusters, but significantly higher than it is in the field today; however, the data sets used were quite small. More recently, Poggianti et al. (2009) find a large incidence of dusty starburst galaxies for $0.4 < z < 0.8$ in all environments, but particularly in groups. Using an entirely different approach, Bell et al. (2005) find a substantial fraction of massive field galaxies at $z \sim 0.7$ with SFRs much higher than their long-term averages. On the other hand, Noeske et al. (2007) argue that the narrow width of the SFR/mass versus mass relation among field galaxies in the Groth strip of DEEP2 data is inconsistent with a large fraction of strong starbursts.

Determining the SBF as a function of cosmic epoch and environment is important both for understanding the nature and cause of starbursts, and their role in galaxy evolution. For example, starbursts provide a quick means of exhausting the gas supply in a galaxy. The dense environment of rich clusters provides a variety of mechanisms for producing starbursts, including ram pressure from the intergalactic medium, tidal encounters between galaxies, and mergers and accretion. Some of these are also viable in the group environment, to more or less effect, but ram pressure, for example, is likely to be unimportant. Some present-epoch, truly isolated galaxies appear to have experienced starbursts as well, which might point to some instability in the disks of star-forming galaxies, or accretion of a small satellite, as other possible causes.

Figure 2 compares results from two different methods of determining the SBF. The top panel shows the fraction of all galaxies in our field sample that have EW(Hδ) of 2.5 Å or greater than expected for a normal, nonbursting galaxy, following the method of D04, but using an improved EW(Hδ) versus EW([O II]) relation (q.v., Oem09). Following Bell et al. (2005), we also calculate the SBF from the *Spitzer*-derived SFRs, by defining a starburst galaxy as one whose observed SFR is significantly higher than its long-term average rate, which should be, ignoring mass loss during stellar evolution,

$$\mathrm{SFR}_{\mathrm{past\ average}} = M_{\mathrm{gal}}/t_{\mathrm{gal}} = (L_{\mathrm{gal}} \times M/L)/t_{\mathrm{gal}}, \qquad (1)$$

where t_{gal} is the length of time that a galaxy has been forming stars, and M_{gal}, L_{gal}, and M/L are the galaxy's *stellar mass*,

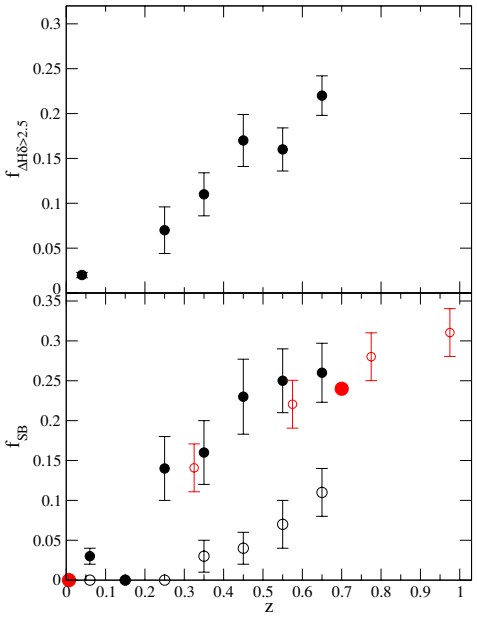

Figure 2. Two measures of starburst fraction vs. redshift for galaxies brighter than M^*+1. Top: fraction of galaxies with excess EW(Hδ) > 2.5 Å; bottom: fraction of galaxies with SFR $> 3 \times L_{\rm tot} \times (M/L)/\tau$(universe). Black filled circles, ICBS data; open red circles, data from Noeske et al. (2007); red filled circles, data from Bell et al. (2005). Black open circles are ICBS data with SFR $> 10 \times L_{\rm tot} \times (M/L)/\tau$(universe). Using this criterion for a starburst, all three samples give consistent results.

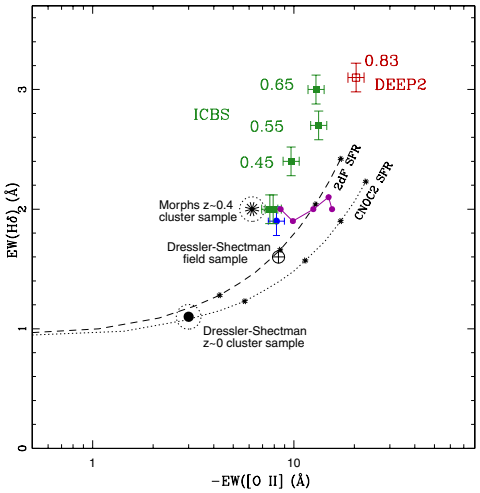

Figure 3. Hδ vs. [O II] equivalent widths for composite spectra, adapted from D04. The lines "2dF" and "CNOC2" show predictions for continuously star-forming populations, and the points "Morphs" and "Dressler–Shectman" cluster and field samples, from studies described in D04. The low-redshift SWIRE field galaxy sample is the blue point. The ICBS field sample measurements are the five green points for redshift intervals centered at $z = 0.25, 0.35, 0.45, 0.55, 0.65$. The five joined purple points show the prediction of EW([O II], Hδ) at these five redshift intervals for a population of present-epoch star-forming galaxies (the SWIRE sample) with very few starbursts, as described in the text. The observed ICBS measurements at $z = 0.45$, 55, and 0.65 far exceed these predicted values, showing the substantial fraction of starburst galaxies in these field populations. The DEEP2 (red) point for field galaxies at $z \sim 0.83$ extends and confirms this result.

luminosity, and stellar mass-to-light ratio, respectively. We define $t_{\rm gal}$ to be the time elapsed from redshift $z = 4$ (a reasonable assumption for the start of star formation) to the observed redshift, and assume that $M_{\rm gal}/L_{\rm gal} = 3$, where $L_{\rm gal}$ is calculated at 4400 Å. We identify a galaxy as a starburst if $\rm SFR_{obs}/SFR_{past\ average} > 3$. We plot in Figure 2 the fraction of galaxies which meet this criterion and perform the same analysis for the observations of Noeske et al. (2007) and Bell et al. (2005). For these we include objects with $M_{\rm gal} \geqslant 1.6 \times 10^{10}\ M_\odot$, which for $M/L = 3$, is equivalent to our luminosity limit of $M^*_{44} + 1.0$.

Figure 2 shows that such starbursts make up ∼20%–25% of star-forming galaxies by $z \sim 0.6$, a much larger fraction than today. Moreover, because the "duty cycle" (fraction of the time these galaxies are identifiable as starbursts) is almost certainly less than 50%, the clear implication is that most star-forming galaxies at $z > 0.6$ have undergone a starburst of at least moderate strength. Figure 2 also shows the SBF for a factor of 10 increase rising in parallel.

Noeske et al. (2007) emphasize the rarity of starbursts over a comparable (but somewhat wider) redshift range, basing their argument on the narrowness of the SFR/M versus M relation. They conclude that no more than one-third of typical star-forming galaxies have SFR variations greater than a factor of 2, while our sample suggests, after correction for the fraction of passive galaxies, that one-third have experienced a rise of a factor of 3 or more. Put in these terms, the two results appear mildly inconsistent, however, as Figure 2 illustrates, the Noeske et al. data, when analyzed using the same method as we and Bell et al. (2005) have used, is in good agreement with our own.

Finally, we show another way of assessing the SBF(z), using the composite spectra approach developed in D04. Here we add, weighted by luminosity, all ICBS spectra in each of the five redshift slices $0.20 < z < 0.70$, and for a present-epoch sample of SWIRE galaxies. We plot in Figure 3 EW([O II], Hδ) measured from these composite spectra, along with expected values for a population of (mostly) continuously star-forming galaxies at the present epoch. Figure 3 includes expected values calculated by D04 from the 2dF and CNOC2 field surveys (see D04) and also new determinations using the SWIRE data, an improvement because we now have individual [O II] distributions (on which these predictions rest) from our ICBS sample, for each redshift interval. The Dressler–Shectman low-redshift cluster and field samples follow the "continuous star formation" prediction, but the clusters at $z \sim 0.4$ studied in the Morphs collaboration depart, indicating a higher fraction of starbursts (see D04).

For the new field sample, Figure 3 shows that the $z = 0.25, 0.35$ slices are little different from the present-epoch population, but the $z = 0.45, 0.55, 0.65$ slices have much stronger Hδ absorption than expected for a population dominated by continuous star formation. We can also compare our EW([O II], Hδ) values to those from a composite spectrum of ∼1000 field galaxies at $z \sim 0.8$ from the DEEP2 Galaxy Redshift Survey (Davis et al. 2007). This co-added spectrum was produced as described in Weiner et al. (2009) by Jeff Newmann and Renbin Yan from galaxies selected with limiting M_R comparable to our own sample. The DEEP2 point continues the trend of yet greater SBF to even higher redshift, for a data set independent of our own, with higher S/N and higher spectral resolution.

In summary, methods based on (1) individual Hδ strengths, (2) the SFR-increase-over-past-average, and (3) (EW([O II], Hδ) from composite spectra, all point to an SBF that increases markedly with redshift.

5. DISCUSSION AND CONCLUSIONS

We have used optical spectra and mid-IR fluxes of field galaxies in our ICBS galaxy cluster survey to measure the rapid decline of the specific star formation rate (SFR) since

$z \sim 0.7$. Although qualitatively consistent with other studies, we find that—parameterized as the median specific SFR—this decline appears to be steepening toward the present epoch. This might be evidence for a kind of "downsizing:" elliptical/bulge formation dominates at $2 < z < 6$ and smoothly transitions to the building of massive galaxy disks, but as this wanes for $z < 1$, there is insufficient mass in the still-star-forming dwarf galaxy population to prevent what is essentially the end of the era of star formation (Dressler 2004).

We also show that it is not just the SFR, but also its mode—the starburst fraction—that is evolving rapidly since $z = 0.7$. We use three different methods, from discrete and composite spectra, to show that the SBF also declines dramatically over this period. When accounting for the "duty cycle," the data suggest that the *majority* of star-forming galaxies at $z \gtrsim 0.5$ followed this mode of star formation rather than in the steadier, "continuous" mode that dominates today. We emphasize that, unlike short and often-intense nuclear starbursts, these are typically of moderate strength—the SFR rising by a factor of 3–10. They are likely to be galaxy-wide and of longer duration—consistent with the dynamical timescales of the larger region involved.

It seems possible that these two effects—the rapid decline in specific SFR and the changing mode of star formation—share a common cause. Availability of gas for star formation could be the principal agent. If the Schmidt–Kennicutt (Kennicutt 1998) law holds, higher SFRs of intermediate-redshift galaxies were due to gas fractions higher than the 20%–40% typical of today's luminous spirals (McGaugh & de Blok 1997), although how much greater may depend on the relative importance of H_2 versus H I (Robertson & Kravtsov 2008; Krumholz et al. 2009). As discussed by Putnam et al. (2008), this greater gas content could be due to initial supply, accretion of gas-rich satellites, or resupply from surrounding reservoirs of cooling gas, the latter the subject of much recent discussion (see, e.g., Keres et al. 2009). However, direct measurements of gas contents for intermediate-redshift galaxies are not yet possible, and absorption measurements by Prochaska & Wolfe (2009)—albeit of H I alone—support a different picture in which gas fractions do not evolve strongly and high SFRs are instead supported by high rates of gas accretion.

If higher SFRs were the result of higher gas fractions of more than 50% for typical $z > 0.5$ galaxies, then it is reasonable to suppose that the higher SBF might also be a result. Star formation in gas-rich disks may be unstable if high supernovae rates heat disks sufficiently to disrupt conditions favorable for star formation. After a gas-cooling time of several hundred million years, rapid star formation could return: color–magnitude diagrams for some nearby dwarf galaxies show two or more episodes of star formation separated by billions of years (e.g., Gallart et al. 1999; Held et al. 2000). If resupply by cold gas flows is important to the evolution of spiral disks, the higher infall rates of earlier epochs could be subject to significant variability, simply a result of the granularity of the gas density in a complex network of filaments.

Finally, mergers of gas-rich galaxies might contribute to the rising SBF with increasing redshift, although Bell et al. (2005) find only a small fraction of their high SFR galaxies at $z \sim 0.7$ in major mergers. Perhaps a higher rate of accretion of small satellites at earlier times might have resulted in more starbursts. Indeed, since these smaller systems were probably gas rich, accretion rather than major mergers might be the dominant starburst trigger.

As yet there are no direct means to measure gas fractions in $z \sim 1$ galaxies, but ALMA and the proposed Square Kilometer Array will in future provide that capability. Until that time, there is an important role for numerical modeling, with its increasing resolution, to explore whether gas fractions, inflow rates, and satellite accretion would affect not just the rate of star formation but its mode as well.

Dressler and Oemler acknowledge support of the NSF grant AST-0407343. All the authors thank NASA for its support through NASA-JPL 1310394. Jane Rigby is supported by a *Spitzer Space Telescope* Postdoctoral Fellowship. Partial support was also provided through contract 1255094 from JPL/Caltech to the University of Arizona. The authors gratefully acknowledge Jeff Newman, Renbin Yan, and the DEEP2 team for the composite spectrum used in this Letter.

Facilities: Spitzer (MIPS), Magellan:Baade (IMACS), Magellan:Clay (LDSS3)

REFERENCES

Blanton, M. R., et al. 2003, ApJ, 592, 819
Bell, E. F., et al. 2005, ApJ, 625, 23
Bouwens, R. J., Illingworth, G. D., Franx, M., & Ford, H. 2008, ApJ, 686, 230
Butcher, H., & Oemler, A., Jr. 1978, ApJ, 279, 18
Couch, W. J., & Sharples, R. M. 1987, MNRAS, 229, 423
Damen, M., Labbe, I., Franx, M., van Dokkum, P. G., Taylor, E. N., & Gawiser, E. J. 2009, ApJ, 690, 937
Davis, M., et al. 2007, ApJ, 660, 1
Donley, J. L., Rieke, G. H., Pérez-González, P. G., & Barro, G. 2008, ApJ, 687, 111
Dressler, A. 2004, in Clusters of Galaxies: Probes of Cosmological Structure and Galaxy Evolution, from the Carnegie Observatories Centennial Symposia, ed. J. S. Mulchaey, A. Dressler, & A. Oemler (Cambridge: Cambridge Univ. Press), 207
Dressler, A., & Gunn, J. E. 1983, ApJ, 270, 7
Dressler, A., Oemler, A., Jr., Poggianti, B. M., Smail, I., Trager, S. C., Shectman, S. A., Ellis, R. S., & Couch, W. J. 2004, ApJ, 617, 867 (D04)
Dressler, A., Rigby, J., Oemler, A., Jr., Fritz, J., Poggianti, B. M., Rieke, G., & Bai, L. 2009, ApJ, 693, 140
Fall, S. M., Charlot, S., & Pei, Y. C. 1996, ApJ, 464, L43
Gallart, C., Freedman, W. L., Aparicio, A., Bertelli, G., & Chiosi, C. 1999, AJ, 118, 2245
Giavalisco, M., et al. 1994, ApJ, 600, 103
Held, E. V., Saviane, I., Momany, Y., & Carraro, G. 2000, ApJ, 530, 88
Hopkins, A. M., & Beacom, J. F. 2006, ApJ, 651, 142
Kennicutt, R. C., Jr. 1998, ARA&A, 36, 189
Keres, D., Katz, N., Dave, R., Fardal, M., & Weinberg, D. H. 2009, MNRAS, 395, 160
Krumholz, M. R., McKee, C. F., & Tumlinson, J. 2009, arXiv:0904:0009
Lilly, S. J., Le Fevre, O., Hammer, F., & Crampton, D. 1996, ApJ, 460, L1
Lonsdale, J. L., et al. 2003, PASP, 115, 897
Madau, P., Pozzeitti, L., & Dickinson, M. 1998, ApJ, 498, 106
Martin, D. C., et al. 2007, ApJS, 173, 415
Noeske, K. G., et al. 2007, ApJ, 660, L43
Oemler, A., Jr., Dressler, A., Kelson, D., Rigby, J., Poggianti, B. M., Fritz, J., Morrison, G., & Smail, I. 2009, ApJ, 693, 152 (Oem09a)
Pérez-González, P. G., et al. 2006, ApJ, 648, 987
Pérez-González, P. G., et al. 2008, ApJ, 675, 234
Poggianti, B. M., Smail, I., Dressler, A., Couch, W. J., Barger, A. J., Butcher, H., Ellis, R. S., & Oemler, A., Jr. 1999, ApJ, 518, 576
Poggianti, B. M., et al. 2009, ApJ, 693, 112
Prochaska, J. X., & Wolfe, A. M. 2009, ApJ, 696, 1543
Putnam, M. E., et al. 2009, arXiv:0902.4717
Rieke, G. H., Alonso-Herrero, A., Weiner, B. M., Pérez-González, P. G., Blaylock, M., Donley, J. L., & Marcillac, D. 2009, ApJ, 692, 556
Robertson, B. E., & Kravtsov, A. V. 2008, ApJ, 680, 1083
Schiminovich, D., et al. 2005, ApJ, 619, 47
McGaugh, S. S., & de Blok, W. J. G. 1997, ApJ, 481, 689
Villar, V., Gallego, J., Pérez-González, P. G., Pascual, S., Noeske, K., Koo, D. C., Barro, G., & Zamorano, J. 2008, ApJ, 677, 169
Weiner, B. J., et al. 2009, ApJ, 693, 187
Zheng, X. Z., Bell, E. F., Papovich, C., Wolf, C., Meisenheimer, K., Rix, H.-W., Rieke, G., & Somerville, R. 2007, ApJ, 661, 41